Solid State Sciences 67 (2017) 1–7

Contents lists available at ScienceDirect

Solid State Sciences

journal homepage: www.elsevier.com/locate/ssscie

Thermal, dielectric and barocaloric properties of NH_4HSO_4 crystallized from an aqueous solution and the melt

E.A. Mikhaleva [a, *], I.N. Flerov [a, b], A.V. Kartashev [a, c], M.V. Gorev [c, b], E.V. Bogdanov [a, d], V.S. Bondarev [a, b]

[a] Kirensky Institute of Physics, Federal Research Centre, KSC SB RAS, 660036, Krasnoyarsk, Russia
[b] Siberian Federal University, 660074 Krasnoyarsk, Russia
[c] Astafijev Krasnoyarsk State Pedagogical University, 660049 Krasnoyarsk, Russia
[d] Krasnoyarsk State Agrarian University, 660049 Krasnoyarsk, Russia

ARTICLE INFO

Article history:
Received 18 October 2016
Received in revised form
13 February 2017
Accepted 6 March 2017
Available online 7 March 2017

Keywords:
Ferroelectric
Phase transition
Thermal and dielectric properties
Entropy
Phase diagram

ABSTRACT

A study of heat capacity, thermal dilatation, permittivity, dielectric loops and susceptibility to hydrostatic pressure was carried out on quasi-ceramic samples of NH_4HSO_4 obtained from an aqueous solution as well as the melt. The main parameters of the successive $P2_1/c$ (T_1) ↔ Pc (T_2) ↔ $P1$ phase transitions did not depend on the method of preparation of the samples, and were close to those determined in previous studies of single crystal and powder, except for the sign and magnitude of the baric coefficient for T_2. Direct measurements of the pressure effect on the permittivity and thermal properties showed $dT_2/dp = -123$ K·GPa^{-1}, which is consistent in terms of magnitude and sign with the baric coefficient evaluated using dilatometric and calorimetric data in the framework of the Clausius-Clapeyron equation. Thus, the temperature region of the ferroelectric Pc phase existence is extended under pressure. A strong decrease in the entropy jump at the Pc ↔ $P1$ transformation with an increase in pressure, and the linear dependence of T_2 on pressure, indicate that an increase in pressure shifts this phase transition towards the tricritical point on the T–p phase diagram. A significant barocaloric effect was found in the region of the Pc ↔ $P1$ phase transition.

© 2017 Elsevier Masson SAS. All rights reserved.

1. Introduction

In spite of the fact that ferroelectric properties were discovered in ammonium hydrogen sulphate, NH_4HSO_4, many years ago [1] and have been actively studied, this compound is currently still of interest to investigators. The most important features of NH_4HSO_4 are as follows: firstly, the existence of spontaneous polarization in a restricted temperature range of between $T_1 = 270$ K and $T_2 = 154$ K [1]; secondly, piezoelectric properties which exist below T_1 down to at least 77 K [1]; thirdly, the possibility of being grown from the melt as well as from an aqueous solution [2]; and fourthly a T–p phase diagram which is rich in pressure-induced phases [3–5]. The crystal structure and mechanism of structural distortions in ammonium hydrogen sulphate have been repeatedly discussed using the results of X-ray, neutron, NMR and Raman scattering investigations [1,5–9]. The main conclusions of these studies can be formulated as follows. Successive phase transitions in NH_4HSO_4 are associated with symmetry lowering $P2_1/c$ (T_1) ↔ Pc (T_2) ↔ $P1$ (in all phases $Z = 8$) upon cooling, and belong to the order-disorder transformations. At temperatures above T_1, there are two kinds of crystallographically nonequivalent HSO_4^- ions, one of which is orientationally disordered between two sites and the other of which is ordered. Below T_1 and T_2, all the sulphate groups are completely ordered. Thus, the entropy change associated with the $P2_1/c$ ↔ Pc transformation can be presented as $\Delta S_1 = R \frac{1}{2} \ln 2 = 2.9$ J·(mol·K)$^{-1}$, which is comparable with the experimental values $\Delta S_1 = (1.7–2.2)$ J (mol·K)$^{-1}$ [1,10,11]. The structural distortion at T_2 is driven by the tilting of the NH_4^+ tetrahedra as well as large changes in the S–O stretching and bending vibrational modes [8,9]. This solely qualitative characterization of the mechanism of the symmetry change does not allow a simple calculation of the entropy change at the Pc ↔ $P1$ phase transition. However, the large

* Corresponding author.
E-mail addresses: katerina@iph.krasn.ru (E.A. Mikhaleva), flerov@iph.krasn.ru (I.N. Flerov), akartashev@yandex.ru (A.V. Kartashev), gorev@iph.krasn.ru (M.V. Gorev), evbogdanov@iph.krasn.ru (E.V. Bogdanov), vbondarev@yandex.ru (V.S. Bondarev).

http://dx.doi.org/10.1016/j.solidstatesciences.2017.03.004
1293-2558/© 2017 Elsevier Masson SAS. All rights reserved.

value of $\Delta S_2 = (6.7–8.8)$ J (mol·K)$^{-1}$ found in calorimetric experiments [1,10] suggests pronounced structural changes.

The effect of internal chemical and external pressure on the phase transition temperatures T_1 and T_2 were examined using Rb → NH_4 cationic substitution [12,13] and in studies of dielectric properties under hydrostatic pressure [4,14]. In the former case, the study of the $(NH_4)_{1-x}Rb_xHSO_4$ solid solutions revealed a strong decrease in T_2 with increase of the rubidium concentration [13]. Compounds with $x \geq 0.33$ undergo only a single transformation $P2_1/c \leftrightarrow Pc$ at a temperature which is rather close to T_1 in NH_4HSO_4. An increase in the hydrostatic pressure induces thinning of the intermediate ferroelectric phase due to the strong differences between the baric coefficients dT_1/dp = 140 K/GPa and dT_2/dp = 765 K/GPa [4,14]. At room temperature and $p > 0.15$ GPa, the crystal structure of NH_4HSO_4 is assumed to be triclinic $P1$.

Since the ionic radius of the rubidium atom exceeds that of the ammonium group, it could be supposed that the Rb → NH_4 substitution would increase the unit cell volume V_{cell} in the $P2_1/c$ phase. It is therefore interesting that there is no strong evidence for the effect of the Rb → NH_4 cationic substitution on the V_{cell} value in the initial paraelectric $P2_1/c$ phase. According to various data, the unit cell volume of NH_4HSO_4 (V_{cell} = (840.6–847.6) Å^3) [1,6,7,9] has been determined to be either less or more than that in $RbHSO_4$ ((838.7–844.5) Å^3) [12,15–17].

Moreover, since the Rb → NH_4 substitution is accompanied by a markedly different relative change in the unit cell parameters: $\Delta a/a = -1.1\%$, $\Delta b/b = +1.7\%$, $\Delta c/c = -0.6\%$ [1,12], the change of internal chemical pressure is not isotropic. Thus, the absence of the $Pc \leftrightarrow P1$ phase transition in $RbHSO_4$ is likely to be associated not with the decrease in chemical pressure but with the absence of the ammonium ion which plays a significant role in the mechanism of related structural distortions in NH_4HSO_4 [8,9].

Attention should also be paid to the ratio between the values of V_{cell} at different temperatures in the three phases of NH_4HSO_4 [1,9] (Fig. 1). According to the data for the volume coefficient of the thermal dilatation β measured between T_2 and room temperature [18], the β value changes only slightly in this temperature range, and the β anomaly at T_1 is rather small. Thus, to a first approximation, it can be assumed that the $V_{cell}(T)$ dependence is close to the linear behaviour between room temperature and T_2, as shown in Fig. 1.

The average β values obtained from Fig. 1 (~$2.5 \cdot 10^{-4}$ K^{-1}) and experimentally determined in Ref. [18] ($2 \cdot 10^{-4}$ K^{-1}) are close to each other. Far below the phase transition $Pc \leftrightarrow P1$ (T_2–30 K), the experimentally determined V_{cell} remains close to the value at 200 K [1,9] and exceeds V_{cell} at T_2 obtained from the linear extrapolation

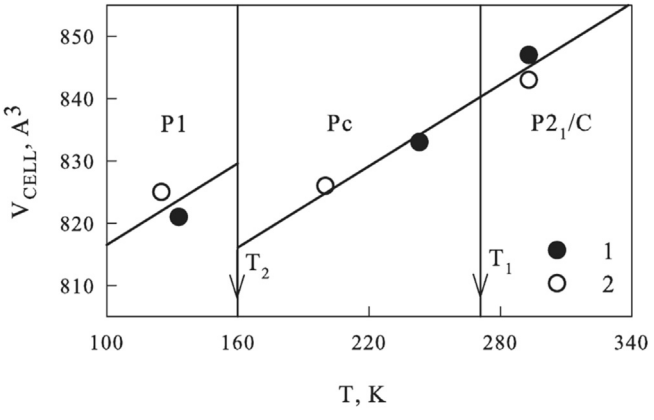

Fig. 1. Ratio between the unit cell volumes V_{cell} in the three phases of NH_4HSO_4. 1 - [1], 2 - [9].

of the $V_{cell}(T)$ dependence from the Pc phase. Fig. 1 clearly shows that at T_2, the volume of NH_4HSO_4 decreases upon heating from the $P1$ phase to the Pc phase. Below T_2 the character of the V_{cell} changes with temperature was chosen as the same for $T > T_2$. Since the entropy increases with an increase in temperature $S_{Pc} > S_{P1}$ at the $P1 \leftrightarrow Pc$ phase transition, the baric coefficient should be negative, in accordance with the Clausius-Clapeyron equation, $dT_2/dp = \delta V/\delta S$. This means that the hydrostatic pressure stabilizes the ferroelectric phase Pc, leading to an expansion of the temperature interval of this phase. However, the authors of [4,14] did not address the contradiction between this fact and the positive sign of the value for dT_2/dp presented in their papers.

Since we intend to explore in future the effect of restricted geometry on the properties of NH_4HSO_4 embedded from the melt into nanoporous boron-silicate glass matrices, it was necessary to obtain reliable information on its properties, including the susceptibility to hydrostatic pressure of a “free” bulk ferroelectric sample. On the one hand, embedding from the melt allows one to obtain a high filling degree; on the other, to the authors' knowledge, all previous studies of ammonium hydrosulphate have been performed on samples prepared from an aqueous solution. Therefore, in this work, two types of polycrystalline NH_4HSO_4 samples were examined: the first was crystallized from an aqueous solution, and the second was obtained after melting the first sample. Hereinafter, these samples will be labelled as AHS Sol and AHS Melt, respectively.

2. Experimental

Small single crystals of AHS Sol were obtained by slow evaporation at 45 °C from an aqueous solution containing equimolar quantities of $(NH_4)_2SO_4$ and H_2SO_4. The AHS Melt sample was prepared by melting at about 160 °C the compound synthesized from a water solution.

The quality of both samples used for the experiments was checked at room temperature using XRD, which revealed a monoclinic symmetry consistent with the space group $P2_1/c$ ($Z = 8$) suggested in Refs. [1,6,7,9]. No additional phases were observed in the samples. Fig. 2 shows the results of Rietveld refinement for both AHS Sol and AHS Melt.

The unit cell parameters in both samples (AHS Sol: a = 24.770(6) Å, b = 4.611(1) Å, c = 14.871(4) Å, β = 89.70(1) grad; AHS Melt: a = 24.7021(9) Å, b = 4.5961(1) Å, c 14.8357(6) Å, β = 89.871(3) grad) are consistent with each other as well as with the values determined in Refs. [1,9].

All measurements were performed on the same samples of AHS Sol and AHS Melt, prepared as quasi-ceramic disc-shaped pellets of 8 mm diameter and 1.3 mm thickness without heat treatment due to the presence of ammonium ions. For dielectric measurements, silver electrodes were painted onto the pellets' surfaces.

In the first stage, thermal dilatation was studied in a temperature range from 100 to 350 K with a heating rate of 3 K/min using a NETZSCH model DIL-402C pushrod dilatometer. Measurements were performed in a dry He flux. The thermal expansion of the system was taken into account using the results of a calibration carried out with quartz as the standard reference. The uncertainty in thermal expansion measurements was about 5%.

The temperature evolution of the heat capacity $C_p(T)$ of both samples was recorded in a wide temperature range of 80–290 K by means of a homemade adiabatic calorimeter with uncertainty in the value of C_p of less than 0.5%–1.0% [19]. Both continuous and discrete heating was used to measure the heat capacity of the system, made up of the sample, heater and contact grease. In the former case, the system was heated at rates of $dT/dt \approx 0.15–0.30$ K/min; in the latter case, the calorimetric step was varied from 1.5 to

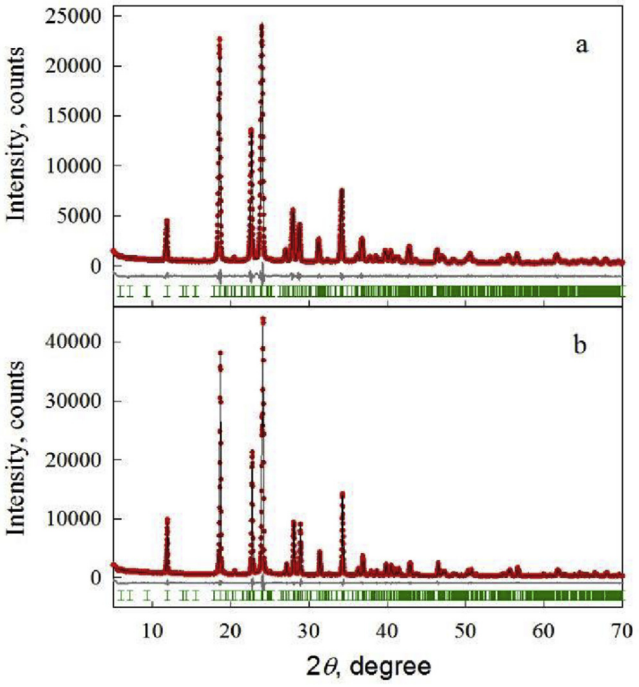

Fig. 2. Difference Rietveld plots of (a) AHS Sol and (b) AHS Melt.

3.0 K. The heat capacities of the heater and contact grease were measured in individual experiments.

Dielectric measurements were also carried out in an adiabatic calorimeter. The permittivity ε was studied using an E7-20 immittance meter at frequencies from 250 Hz up to 10^6 Hz while heating at a rate of about 0.5 K/min. The dielectric hysteresis (P–E loop) was examined using an aixACCT EASY CHECK 300 technique. The driving-field profile was a triangular wave of amplitude $E_{max} = 3$ kV/cm. The frequency of the measuring electric field was 250 Hz.

The investigations of the susceptibility of the phase transition temperatures in NH_4HSO_4 to hydrostatic pressure were carried out using a piston-cylinder type vessel associated with a pressure multiplier. Pressure of up to 0.25 GPa was generated using pentane as the pressure-transmitting medium. Pressure and temperature were measured using a manganin gauge and a copper-constantan thermocouple, with accuracies of about $\pm 10^{-3}$ GPa and ±0.3 K respectively.

Because the phase transition at T_2 is of first order, accompanied by a large entropy change and a reliably detected stepwise change in permittivity [1,10], the baric coefficient dT_2/dp could be determined by measuring both permittivity and the differential thermal analysis (DTA) signal. In the latter case, a sample was glued onto one of the two junctions of a germanium-copper thermocouple characterized by high sensitivity to changes in temperature. A quartz sample cemented to the other junction was used as a reference substance. To ensure the reliability of the results, the measurements were performed for both increasing and decreasing pressure cycles.

The high-temperature transformation is a typical second order transformation with a relatively small change in heat capacity at T_1 [1,10]. Therefore the dT_1/dp value was determined mainly from the permittivity measurements under pressure.

Error bars on all experimental and calculated data were determined taking into account the uncertainty in the measurement of the basic quantities (temperature, pressure, heat capacity and thermal expansion).

3. Results and discussion

The results of the dilatometric studies presented in Fig. 3 show that the temperature evolution of the linear strain $\Delta L/L_0$ is the same for AHS Sol and AHS Melt.

The second order phase transition at $T_1 = 273 \pm 2$ K was detected as a small deviation from the monotonous increase of $\Delta L/L_0$ with temperature. In accordance with the first order $P1 \leftrightarrow Pc$ transformation, strong anomalous behaviour in the linear strain was observed in the narrow temperature range around T_2. The values of the temperature $T_2 = 165 \pm 1$ K and the negative strain jump $\delta(\Delta L/L_0)_{T=T2} = -(0.50 \pm 0.02)\%$ were found to be the same for both samples. The volume strain change for quasi-ceramic samples was determined as $\delta(\Delta V/V_0)_{T=T2} = 3\delta(\Delta L/L_0)_{T=T2} = -(1.50 \pm 0.07)\%$. This value gives the dominant contribution to the total change in the volume strain $\delta(\Delta V/V_0)_{T=T2}/\Delta(\Delta V/V_0) = 0.87 \pm 0.05$ and clearly indicates that the $P1 \leftrightarrow Pc$ phase transition is far from the tricritical point where $\delta(\Delta V/V_0) \to 0$. The results obtained agree well with those presented in Refs. [1,9] and Fig. 1, showing that the volume of NH_4HSO_4 decreases upon heating through the $P1 \leftrightarrow Pc$ transformation. This means that in accordance with the Clausius-Clapeyron equation, hydrostatic pressure should decrease the temperature T_2, contrary to the increase associated with the large positive baric coefficient dT_2/dp proposed in previous experiments [4,14]. It is interesting to note that a negative change upon heating was also found in the linear strain along the ferroelectric c axis of the NH_4HSO_4 single crystal [10].

The data obtained by adiabatic calorimeter are shown in Fig. 4a. Two anomalies in heat capacity were observed at temperatures $T_1 = 270.5 \pm 0.5$ K and $T_2 = 159.0 \pm 0.5$ K; these are somewhat lower than those determined in dilatometric measurements, as in the latter case, the rate of the temperature variation was higher. On the other hand, both phase transition temperatures agree well with the T_1 and T_2 values determined in heat capacity measurements of a single crystal of NH_4HSO_4 [10].

As was observed in the dilatometric measurements, calorimetric experiments also revealed a small stepwise anomaly at T_1, characteristic of the second order transition, and a very large peak of the heat capacity at T_2, associated mainly with the enthalpy (entropy) jump at a strong first order phase transformation.

In order to obtain information on the integral thermodynamic characteristics of phase transitions such as enthalpy and entropy changes, the anomalous, ΔC_p, and lattice, C_L, contributions to the total heat capacity C_p were separated. This procedure was carried out using a simple model describing C_L. The experimental data taken far from the transition points ($T < 145$ K and $T > 272$ K) were

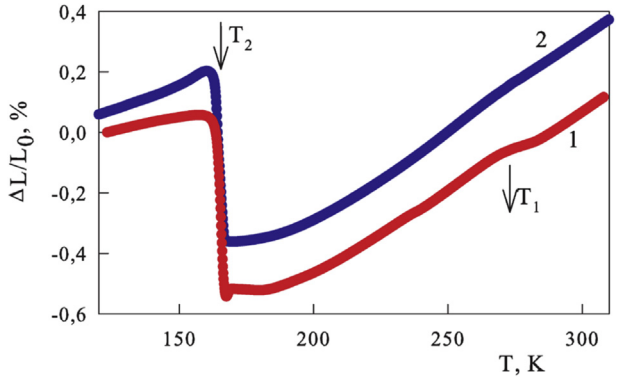

Fig. 3. Temperature dependence of the linear strain in (1) AHS Sol and (2) AHS Melt.

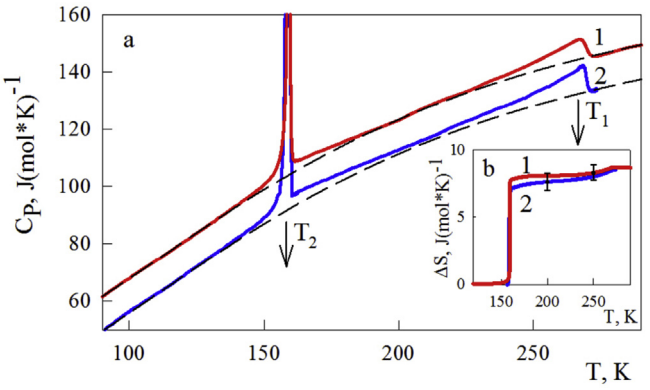

Fig. 4. (a) Temperature dependence of the molar heat capacity of AHS Sol (1) and AHS Melt (curve 2 is shifted down at 12 J (mol K)$^{-1}$. The dashed line is the lattice heat capacity; (b) Temperature dependence of the excess entropy associated with the $P2_1/c \leftrightarrow Pc \leftrightarrow P1$ phase transitions.

fitted using a linear combination of Debye and Einstein terms $C_L = K_D C_D + K_E C_E$, where

$$C_D(T) = 9R\left(\frac{T}{\Theta_D}\right)^3 \int_0^{\frac{\Theta_D}{T}} \frac{x^4 \exp(x)}{(\exp(x)-1)^2} dx$$

$$C_E(T) = 3R\left(\frac{\Theta_E}{T}\right)^2 \frac{\exp(\Theta_E/T)}{(\exp(\Theta_E/T)-1)^2}$$

and K_D, K_E, Θ_D, Θ_E are fitting parameters.

The average deviation of the experimental data from the smoothed curves does not exceed 0.5%. The lattice contribution is shown as a dashed line in Fig. 4a. It can be seen that at T_1 the smearing of ΔC_p associated with the ceramic nature of the samples was observed only within the narrow temperature interval $T_1 + 3$ K. In the *Pc* phase, the anomalous contribution ΔC_p exists far below T_1 in accordance with the polarisation behaviour $\Delta C_p \sim (\partial \Delta S/\partial T)_p \sim (\partial P^2/\partial T)_p$ [1,10].

The enthalpies of the phase transitions were determined by integrating the $\Delta C_p(T)$ function: AHS Sol - $\Delta H_1 = 260 \pm 25$ J·mol^{-1} and $\Delta H_2 = 1230 \pm 130$ J·mol^{-1}; AHS Melt - $\Delta H_1 = 300 \pm 45$ J·mol^{-1} and $\Delta H_2 = 1160 \pm 110$ J·mol^{-1}.

Fig. 4b shows the temperature behaviour of excess entropy associated with the successive phase transitions in both AHS Sol and AHS Melt, calculated by integrating the area below the $\Delta C_p/T$ versus T curves. It can be seen that there is a difference between these two curves. However, taking into account the uncertainty in the heat capacity measurements as well as the choice of C_{lat}, the values of the entropy changes are close to each other (AHS Sol - $\Delta S_1 = 1.15 \pm 0.11$ J·(mol·K)$^{-1}$, $\Delta S_2 = 7.7 \pm 1.0$ J·(mol·K)$^{-1}$; AHS Melt - $\Delta S_1 = 1.35 \pm 0.17$ J·(mol·K)$^{-1}$, $\Delta S_2 = 7.2 \pm 0.8$ J·(mol·K)$^{-1}$) and are comparable with the entropies determined for a single crystal of NH_4HSO_4 ($\Delta S_1 = 1.7 \pm 0.20$ J·(mol·K)$^{-1}$, $\Delta S_2 = 6.7 \pm 0.7$ J·(mol·K)$^{-1}$) [10]. The ratio between the jump δS_2 (AHS Sol—7.2 ± 0.5 J·(mol·K)$^{-1}$; AHS Melt—6.6 ± 0.6 J·(mol·K)$^{-1}$) and the total change in the entropy $\delta S_2/\Delta S_2 \approx 0.93$ is close to the value of $\delta(\Delta V/V_0)_{T=T2}/\Delta(\Delta V/V_0)$ shown above, and can be considered as additional evidence for the significant distance of the first order $Pc \leftrightarrow P1$ phase transition from the tricritical point.

The permittivity in the quasi-ceramic sample AHS Melt (Fig. 5a and b) exhibits specific features identical to those observed in the $\varepsilon(T)$ dependence for the single-crystal sample [1,20]: a jump at $T_2 = 161 \pm 1$ K and a pronounced peak at $T_1 = 271.4 \pm 0.5$ K. At a low

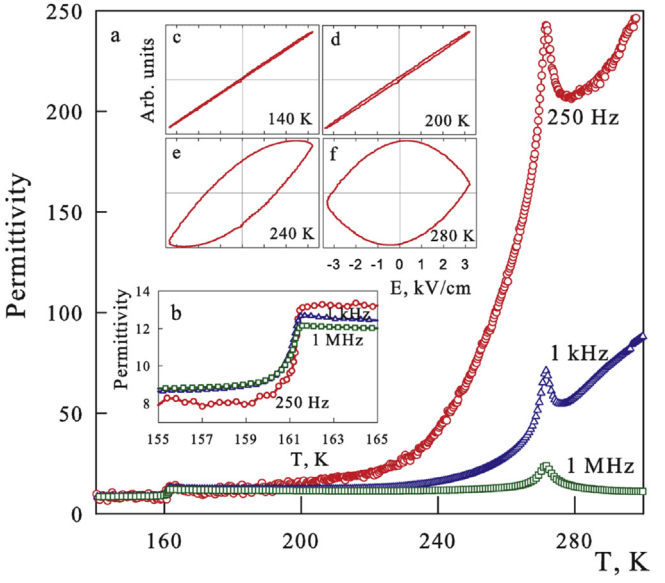

Fig. 5. (a, b) Dependence of permittivity on temperature for AHS Melt at different frequencies; (c, d, e, f) Dielectric hysteresis loops at the corresponding temperatures.

frequency of $f = 250$ Hz, a strong increase of ε was observed above ~190 K from 13 to 250 at 290 K; this decreased with an increase in f of up to 1 MHz.

The behaviour of the ε peak at T_1 and the stepwise change at T_2 were also changed, although to a significantly lesser extent. The temperatures of both phase transitions were not affected by the frequency variation and agreed well with those found in calorimetric measurements.

We also carried out an investigation of the *P*—*E* loops in three phases. As an example, the results for AHS Melt are shown in Fig. 5c—f; these results confirm that the use of polarization is not the best way to study the effect of hydrostatic pressure on the temperature T_2, as has also been demonstrated for a single crystal of NH_4HSO_4 [14]. Firstly, it was found that there is a rather strong relaxation in the appearance of *P* in the *Pc* phase; an almost linear dependence of polarization versus electric field exists far above T_2 (Fig. 5c and d). Secondly, the non-classically shaped dielectric loops do not allow for the correct determination of polarization. This is associated with the low density of the quasi-ceramic samples prepared without heat treatment, and the high electrical conductivity observed in Ref. [21]. Both of these factors contribute to the quasi-ceramic sample; however, the main role is most likely to be played by the latter.

The results of the hydrostatic pressure effect on the permittivity of both NH_4HSO_4 samples at the phase transitions $P2_1/c \leftrightarrow Pc \leftrightarrow P1$ were found to be similar. The experimental data for AHS Melt obtained at frequency $f = 1$ kHz are presented in Fig. 6.

The temperature-dependent behaviour of permittivity in the region of T_1 is similar to that observed in Refs. [4,14]; the permittivity peak shifts under pressure to a higher temperature and a decreases is shown in the maximum value (Fig. 6a). The corresponding baric coefficient $dT_1/dp = 90 \pm 15$ K·GPa^{-1} is close to that measured in Refs. [4,14] and calculated in Ref. [18].

The $\varepsilon(T, p)$ data for the $Pc \leftrightarrow P1$ transformation (Fig. 6b) show a decrease in T_2 accompanied by the smearing and reduction of the step-wise permittivity anomaly. The observed negative sign of dT_2/dp is in contradiction to the increase in T_2 with pressure proposed by earlier experiments studying the dielectric properties [4,14].

Since the heat capacity of NH_4HSO_4 demonstrated a very large

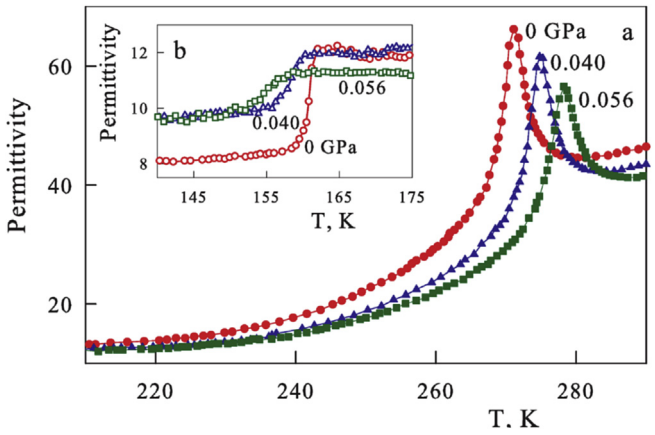

Fig. 6. Temperature dependence of permittivity for AHS Melt measured upon heating at different pressures for the (a) $P2_1/c \leftrightarrow Pc$ and (b) $Pc \leftrightarrow P1$ phase transitions.

anomaly at the low-temperature transformation (Fig. 4), we were able to investigate the pressure effect on the DTA signal associated with the heat effect at T_2. For both AHS Sol and AHS Melt, these experiments revealed firstly a strong shift in T_2 to lower temperatures and, secondly, a decrease of the square under the DTA(T) curves with an increase in pressure (Fig. 7a and b).

Thus, the thermal and dielectric properties of NH_4HSO_4 demonstrate similar behaviour at T_2 under a pressure characterized by the negative baric coefficient.

As usual, the DTA measurements allow the detection of the heat effect associated with the latent heat, or in other words with the jump in enthalpy δH or entropy $\delta S = \delta H/T_{PT}$ at the phase transition point T_{PT}. Because the change in total entropy (as well as in enthalpy) takes place in both samples under study within a very narrow temperature range near T_2, it can be assumed that the DTA experiments above show the decrease in δS_2. This process is accompanied at the same time by the appearance of the temperature- and pressure-dependent part of the excess entropy $\Delta S_2^*(T, p)$ in a certain temperature range, which expands with the pressure.

Thus, the total entropy change $\Delta S_2 = \delta S_2(p) + \Delta S_2^*(T, p)$ remains constant in NH_4HSO_4, at least up to the value of $p \leq 0.23$ GPa realized in our measurements (Fig. 7b). This assumption is a realistic, since it is difficult to imagine that such a low pressure can change the degree of disorder of the structural elements. Thus, a more reasonable and plausible hypothesis is that the increase in pressure induces the approaching of the $Pc \leftrightarrow P1$ transformation to the tricritical point, which is characterised by $\delta H = 0$ and $\delta S = 0$ [22].

We consider the square under the DTA peak at $p = 0$ to be the change in entropy δS determined in experiments with an adiabatic calorimeter. In Fig. 7c and d, a linear decrease can be seen in the changes in entropy in both samples; these are equal to zero at the pressure of the tricritical point, $p_{TCP} \approx 0.17$ GPa in AHS Sol and ~0.24 GPa in AHS Melt. Taking into account the experimental uncertainties, a difference in the p_{TCP} values for different samples can be considered as insignificant.

The experimental results for the pressure effect on both phase transitions in AHS Sol and AHS Melt obtained by measuring ε and δS_2 are summarized on the T–p phase diagram (Fig. 8).

Both properties of the samples under study show the same pressure dependence of T_2 characterized by the negative baric

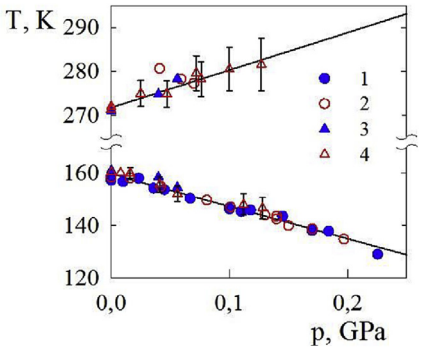

Fig. 8. Temperature–pressure phase diagram combining the results on the DTA signal (1, 2) and permittivity (3, 4) study in AHS Sol (2, 4) and AHS Melt (1, 3).

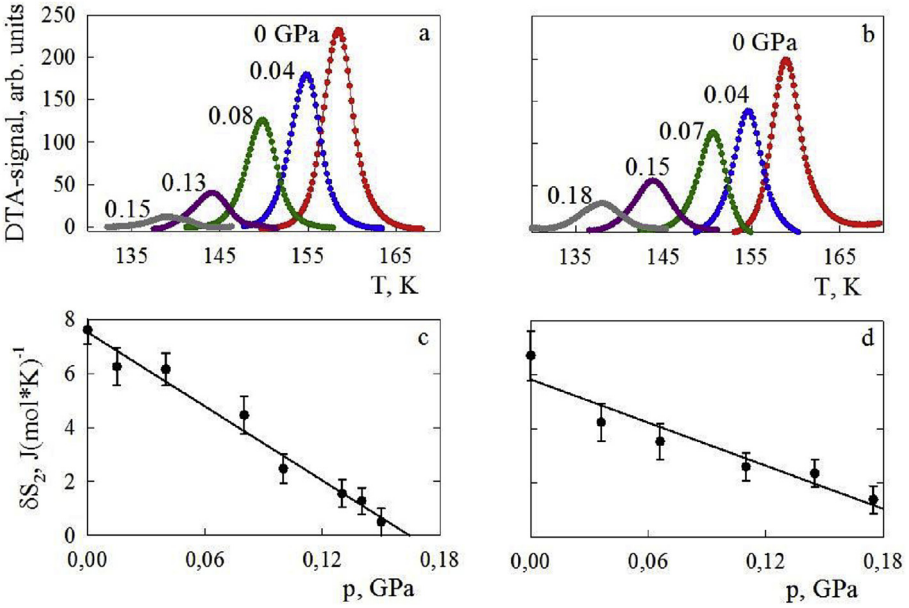

Fig. 7. (a, b) Anomalous component of the DTA signal near T_2 at different pressures in AHS Sol and AHS Melt, respectively; (c, d) Entropy jump δS_2 for the first-order transition in AHS Sol and AHS Melt, respectively. The lines in c and d represent linear fits.

coefficient $dT_2/dp = -123 \pm 15$ K·GPa^{-1}. A shift in T_2 under pressure was also determined using the results of heat capacity and thermal dilatation measurements in the framework of the Clausius-Clapeyron equation $dT_2/dp = \delta V_2/\delta S_2$. These values for AHS Sol (-128 ± 16 K·GPa^{-1}) and AHS Melt (-158 ± 20 K·GPa^{-1}) are close to those obtained by direct measurement of $T_2(p)$.

This good agreement between the data obtained by three independent experiments, carried out on two samples of NH_4HSO_4 prepared by different methods, suggests the high reliability of the determination of the dT_2/dp sign and value.

The reason for the contradiction between these results and the data obtained in Refs. [4,14], where the value for dT_2/dp was found to be positive and very large (+765 K·GPa^{-1}) remains uncertain. This is unlikely to be connected with the type of sample, i.e. the single crystal [4,14] and the quasi-ceramics used in the present study. The temperatures and entropies of the phase transitions $P2_1/c \leftrightarrow Pc \leftrightarrow P1$ and the baric coefficient dT_1/dp in AHS Sol and AHS Melt are in satisfactory agreement with the data obtained for powder [1,5], single crystal [1,9,10,14,23] and ceramic [20] samples. On the other hand, the jump in volume strain $\delta(\Delta V/V_0)$ at T_2, calculated using the Clausius-Clapeyron equation, the baric coefficient dT_2/dp from Refs. [4,14] and the δS_2 value determined in the present paper or in Refs. [1,10] are unrealistically large ~ (+8%). Finally, the positive shift of T_2 under pressure [4,14] stands in contradiction to the negative sign of the volume strain upon heating through the $P1 \leftrightarrow Pc$ phase transition found in the current work (Fig. 3) and in Refs. [1,14].

The constant value of dT_2/dp in both AHS Sol and AHS Melt, at least within the range of pressure studied, means a fall in δV_2 in accordance with a decrease of δS_2. A similar correlated decrease in the volume and entropy changes with pressure was recently observed in $(NH_4)_2SO_4$ undergoing ferrielectric phase transition of the first order, characterized by a negative baric coefficient [24]. It is safe to assume that this transformation is also close to the tricritical point. Certainly, a reduction of δS_2 as well as δV_2 under pressure is not a common feature of phase transitions. For example, recent studies of the $T-p$ phase diagrams in some perovskite-like ferroelastics have shown the change in entropy at the phase transition point to be constant, at least in the range $0 < p < 0.5$ GPa [25,26].

A constant ratio between the values of $\delta S_2(p)$ and $\Delta S_2^*(T, p)$ with a change in pressure is very convenient for the analysis of the barocaloric effect (BCE); this is associated with a decrease in entropy or increase in temperature with an increase in pressure at $T =$ const or $S =$ const, respectively. However, in order to obtain a detailed and correct determination of the BCE in NH_4HSO_4, as well as in recently studied $(NH_4)_2SO_4$ [24], characterized by a decrease in δS_2 and increase in $\Delta S_2^*(T, p)$ with an increase in pressure, it is necessary to have information on the pressure dependence of the heat capacity. Due to a lack of opportunity to measure $C_p(T, p)$, the BCE in $(NH_4)_2SO_4$ was evaluated only in connection with the δS_2 part of the entropy [24]. We were also unable to determine the $\Delta S_2^*(T, p)$ dependence for NH_4HSO_4. However, taking into account that the maximum value of the extensive BCE ΔS_{BCE}^{max} near T_2 is equal to the phase transition entropy ΔS_2, a raw estimation of the minimum pressure, p_{min}, can be made which produces the maximum values of isothermal entropy change ΔS_{BCE}^{max} as well as the adiabatic (AD) temperature change ΔT_{AD}^{max} [26]:

$$p_{min} \geq \frac{T\Delta S_2}{C_p dT_2/dp}$$

$$\Delta T_{AD}{}^{max} = \frac{dT_2}{dp} p_{min}$$

The use of the values for C_p, ΔS_2 and dT_2/dp determined above for AHS Sol and AHS Melt gives $p_{min} = 0.10 \pm 0.02$ GPa and $\Delta T_{AD}^{max} = -12 \pm 2$ K. These are close to the values found for $(NH_4)_2SO_4$ [24]. The negative sign for intensive BCE ($\Delta T_{AD}^{max} < 0$) in both ammonium sulphate and ammonium hydrosulphate (near T_2) is associated with a decrease of the unit cell volume in the region of the phase transition point. On the other hand, both crystals are characterized by the positive volume deformation $\Delta V/V_0 > 0$ far from the transition temperature, which leads to the conventional BCE ($\Delta S_{BCE} < 0$; $\Delta T_{AD} > 0$) in accordance with the Maxwell equation [27]:

$$\left(\frac{\partial S}{\partial p}\right)_T = -\left(\frac{\partial V}{\partial T}\right)_p$$

This feature will decrease the extensive and intensive inverse BCE in the region of the phase transition. Near the $Pc \leftrightarrow P1$ transformation in NH_4HSO_4, these amendments are $-(1.2 \pm 0.2)$ J·(mol·K)$^{-1}$ and $+ (2.0 \pm 0.3)$ K for ΔS_{BCE} and ΔT_{AD}, respectively.

4. Conclusions

A study of the thermal and dielectric properties of two quasi-ceramic samples of NH_4HSO_4 obtained using different methods revealed the following points.

The method of preparation of the samples does not affect the main properties associated with the succession of the $P2_1/c$ (T_1) $\leftrightarrow$ Pc (T_2) $\leftrightarrow$ $P1$ phase transitions. The transformation temperatures, changes of entropy and volume deformation in AHS Sol and AHS Melt are in satisfactory agreement with the data obtained for powder [1,5], single crystal [1,9,10,14,23] and ceramic [20] samples.

Direct dilatometric measurements showed a negative change in the volume deformation at T_2 upon heating; this coincides with the ratio of the unit cell parameters in the Pc and $P1$ phases [1,9].

The temperature-pressure phase diagram, constructed on the basis of the study of the susceptibility of the DTA signal and permittivity to hydrostatic pressure, indicated an expansion of the temperature interval of the stability of the ferroelectric phase Pc associated with the different signs of the baric coefficients dT_1/dp and dT_2/dp. The decrease of T_2 under pressure agrees with the negative sign of $\delta(\Delta V/V)_{T=T2}$. The calculated values of the baric coefficients are close to those obtained by direct measurement.

An increase in pressure leads to a decrease in the change in entropy δS_2 at the $Pc \leftrightarrow P1$ transformation in AHS Sol and AHS Melt; this is connected with the approach of this transformation towards the tricritical point.

The analysis of barocaloric efficiency showed that the maximum extensive and intensive BCE ($\Delta S_{BCE}^{max} = 8 \pm 1$ J (mol·K)$^{-1}$; $\Delta T_{AD}^{max} = 12 \pm 2$ K) can be realized at a relatively low pressure of ~0.1 GPa. The conventional BCE associated with the $Pc \leftrightarrow P1$ phase transition in NH_4HSO_4 does not exceed ~15% of the maximum inverse BCE.

Acknowledgements

We are grateful to T.N. Davydova for the preparation of the sample from an aqueous solution and Dr. M.S. Molokeev for X-ray characterization of the samples. The study was partially supported by the Russian Foundation for Basic Research, research project No. 16-32-00092 mol_a.

References

[1] R. Pepinsky, K. Vedam, S. Hoshino, Y.S. Okaya, Ammonium hydrogen sulfate: a new ferroelectric with low coercive field, Phys. Rev. 111 (1958) 1508–1510.
[2] F. Iona, G. Shirane, Ferroelectric Crystals, Pergamon Press, Oxford, London, New York, Paris, 1962.

[3] P.W. Bridgman, Polymorphism at high pressures, Proc. Am. Acad. Arts Sci. 52 (1916) 91–187.
[4] K. Gesi, K. Ozawa, Pressure-temperature phase diagram of ferroelectric ammonium bisulfate NH_4HSO_4, J. Phys. Soc. Jpn. 43 (1977) 563–569.
[5] L. Bobrowicz, I. Natkaniec, T. Sarga, S.I. Bragin, Neutron scattering studies of pressure induced phase transitions in NH_4HSO_4, High Press. Res. 14 (1995) 61–65.
[6] R.J. Nelmes, An X-ray diffraction determination of the crystal structure of ammonium hydrosulfate above the ferroelectric transition, Acta Crystallogr. B 27 (1971) 272–281.
[7] R.J. Nelmes, The structure of ammonium hydrogen sulfate in its ferroelectric phase and the ferroelectric transition, Ferroelectrics 4 (1972) 133–140.
[8] R. Miller, R. Blinc, M. Brenman, J.S. Waugh, Nuclear spin-lattice relaxation in some ferroelectric ammonium salts, Phys. Rev. 126 (1962) 528–532.
[9] D. Swain, V.S. Bhadram, P. Chowdhury, C. Narayana, Raman and x-ray investigations of ferroelectric phase Transition in NH_4HSO_4, J. Phys. Chem. A 116 (2012) 223–230.
[10] I.N. Flerov, V.I. Zinenko, L.I. Zherebtsova, I.M. Iskornev, D.Ch. Blat, Study of phase transitions in ammonium hydrosulfate, Izvestiya AN USSR (seriya fizicheskaya) 39 (1975) 752–757.
[11] B.A. Strukov, M.N. Danilycheva, Heat capacity of ammonium hydrogen sulfate in the temperature range between −7 and +14 °C, Fiz. Tverd. Tela 5 (1963) 1724–1727.
[12] R. Pepinsky, K. Vedam, Ferroelectric transition in rubidium bisulfate, Phys. Rev. 117 (1960) 1502–1503.
[13] E.A. Mikhaleva, I.N. Flerov, V.S. Bondarev, M.V. Gorev, A.D. Vasiliev, T.N. Davydova, Phase transitions and caloric effects in ferroelectric solid solutions of ammonium and rubidium hydrosulfates, Phys. Solid State 53 (2011) 510–517.
[14] I.N. Polandov, V.P. Mylov, B.A. Strukov, On p–T diagram of ferroelectric crystal NH_4HSO_4, Fiz. Tverd. Tela 10 (1968) 2232–2234.
[15] W.G. Mumme, Alkali metal ordering and hydrogen bonding in the system $KHSO_4$-$RbHSO_4$: the crystal structures of $K_xRb_{1-x}HSO_4$ ($0.3 < x < 0.55$) and $RbHSO_4$, Acta Crystallogr. B 29 (1973) 1076–1083.
[16] J.P. Ashmore, H.E. Petch, The structure of $RbHSO_4$ in its paraelectric phase, Can. J. Phys. 53 (1975) 2694–2702.
[17] K. Itoh, H. Ohno, S.H. Kuragaki, Disordered structure of ferroelectric rubidium hydrogen sulfate in the paraelectric phase, J. Phys. Soc. Jpn. 64 (1995) 479–484.
[18] I.M. Iskornev, I.N. Flerov, Thermal expansion of ferroelectric crystals of the ammonium hydrosulfate family, Fiz. Tverd. Tela 20 (1978) 2649–2653.
[19] A.V. Kartashev, I.N. Flerov, N.V. Volkov, K.A. Sablina, Adiabatic calorimetric study of the intense magnetocaloric effect and the heat capacity of $(La_{0.4}Eu_{0.6})_{0.7}Pb_{0.3}MnO_3$, Phys. Solid State 50 (2008) 2115–2120.
[20] J.E. Diosa, M.E. Fernández, R.A. Vargas, Anomalous phase behaviour of NH_4HSO_4 below room temperature, Phys. Status Sol.(b) 227 (2001) 465–468.
[21] I.N. Flerov, E.A. Mikhaleva, Electrocaloric effect and anomalous conductivity of the Ferroelectric NH_4HSO_4, Phys. Solid State 50 (2008) 478–484.
[22] K.S. Aleksandrov, I.N. Flerov, The region of applicability of the thermodynamic theory of structural phase transitions close to the tricritical point, Fiz. Tverd. Tela 21 (1979) 327–336.
[23] O. Björkström, A. Fredriksson, B.-E. Mellander, J.E. Diosa, R.A. Vargas, Anomalous behaviour of $(NH_4)HSO_4$, Solid State Ionics 69 (1994) 75–77.
[24] P. Lloveras, E. Stern-Taulats, M. Barrio, J.-Ll Tamarit, S. Crossley, W. Li, V. Pomjakushin, A. Planes, Ll Mañosa, N.D. Mathur, X. Moya, Giant barocaloric effects at low pressure in ferrielectric ammonium sulphate, Nat. Commun. 6 (2015) 8801. DOI: 10.1038.
[25] I.N. Flerov, M.V. Gorev, A. Tressaud, N.M. Laptash, Perovskite-like fluorides and oxyfluorides: phase transitions and caloric effects, Crystallogr. Rep. 56 (2011) 9–17.
[26] M.V. Gorev, I.N. Flerov, E.V. Bogdanov, V.N. Voronov, N.M. Laptash, Barocaloric effect near the structural phase transition in the Rb_2KTiOF_5 oxyfluoride, Phys. Solid State 52 (2010) 377–383.
[27] A.M. Tishin, Y.I. Spichkin, The Magnetocaloric Effect and its Applications, Series in Condensed Matter Physics, Institute of Physics Publ., Bristol, Philadelphia, 2003.